Selective excitation via the continuum and suppression of ionization

C. E. Carroll
Department of Physics and Astronomy, University of Rochester, Rochester, New York 14627

F. T. Hioe
Department of Physics, St. John Fisher College, Rochester, New York 14618

(Received 22 July 1992)

Two laser pulses that overlap in time have been successfully used for coherent excitation of a molecule or atom to a desired state. An intermediate state that is at or near resonance with the laser frequencies has been used in past experiments and calculations. Here we replace this intermediate state by a continuum of intermediate states. An analytic solution of a simple model suggests that the continuum can be used in such an excitation scheme, provided that the laser pulses are arranged in the so-called counterintuitive order. We use a special case of this solution to relate this work to ionization suppression and coherent population trapping.

PACS number(s): 32.80.Rm, 33.80.Rv, 42.50.Hz

I. INTRODUCTION

Two stimulated transitions driven by laser beams are often used to transfer molecules to a selected excited state, as in three-state adiabatic passage [1] and stimulated-emission pumping [2]. Use of two laser pulses that overlap in time is a proven method for selective excitation of a molecule [3] or alignment of the angular momentum of an excited atom [4]. It may soon be used for reflection or splitting of an atomic beam [5]. In a three-state model of this process, the molecule or atom is transferred from state 1 to state 3 to state 2 (Fig. 1). Recent measurements [3,4,6] and calculations [7,8] show the advantages of using the "counterintuitive" pulse order [9] in such a case. The two laser pulses are in counterintuitive order if the laser pulse driving the 1-3 transition reaches its peak amplitude *after* the laser pulse driving the 3-2 transition reaches its peak amplitude; the intuitive order must be used if the two laser pulses do not overlap in time. In this paper, we replace state 3 by a continuum of infinitely many states. We calculate the effectiveness of two overlapping laser pulses in driving the molecule or atom from state 1 to state 2 or into the continuum. We suggest that a continuum of intermediate states can be used in stimulated Raman scattering, so that this method of coherent laser excitation will find wider application.

Analytic calculations for a simple model of a molecule or atom driven by two laser pulses are described below.

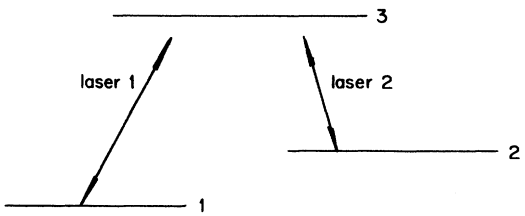

FIG. 1. Three-state model for a stimulated Raman scattering process driven by two laser beams.

A quantum system that has two discrete states and a continuum of states is driven by classical oscillating forces that represent the two laser beams (Fig. 2). A striking difference between intuitive and counterintuitive pulse orders will appear when we calculate the final occupation probabilities. Spontaneous emission of a photon or electron may cause strong damping of the continuum states, but this effect is omitted from our model. We also neglect dephasing of continuum states, and stimulated continuum-continuum transitions. Neglect of these processes may be justified if the continuum states are occupied with low probability for a short time. We shall show that the counterintuitive pulse order can be used to reduce the occupation probability of the continuum. Also, the counterintuitive order makes the transfer process insensitive to small changes in the parameters of the laser pulses. These calculations are given below, along with the calculated distribution of occupation probability in the continuum. This distribution shows another difference between intuitive and counterintuitive pulse orders.

Since we neglect dephasing processes as well as spontaneous emission, the Schrödinger equation can be used

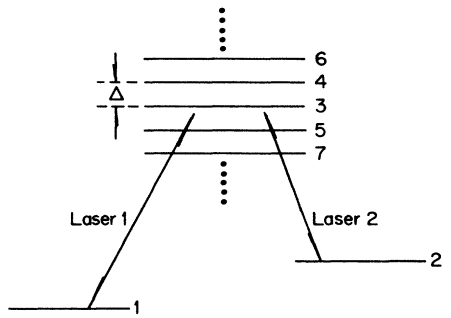

FIG. 2. Uniformly spaced states are used as a model for the continuum that is coupled to states 1 and 2 by laser-driven transitions.

as the equation of motion for our model, which is a quantum system driven by classical oscillating forces. In Sec. II, we set up the Schrödinger equation for a system of N states, and then obtain an analytic solution by using $N\rightarrow\infty$ and some other simplifying assumptions. Only transitions that are driven by nearly resonant oscillating forces are included in this model, for selective excitation is inconsistent with high laser intensities. Because of this, the only continuum states that are significantly populated lie in a narrow band of energies near resonance. This leads us to use a uniform and featureless continuum in our model. However, this continuum model includes states that are arbitrarily far from resonance.

The time-dependent occupation probabilities obtained from this model are discussed in Sec. III, where we find agreement with the golden rule of time-dependent perturbation theory at early times. The growth of the continuum occupation probability is treated in the Appendix. At the end of the two laser pulses, we find final occupation probabilities that are discussed in Sec. IV. The distribution of occupation probability in the continuum is described in Sec. V. The two overlapping laser pulses can be replaced by one rectangular laser pulse, so that all the Rabi frequencies are constant during the pulses. Section VI treats this rectangular pulse shape, which gives results that are intermediate between those for intuitive and counterintuitive pulse pairs. These results connect our calculation to work on coherent population trapping [10,11] and ionization suppression [12–14].

II. SCHRÖDINGER EQUATION AND ITS SOLUTION

The equation of motion for a molecule or atom driven by oscillating external forces is set up and solved in this section. The two laser beams are treated as classical forces acting on the quantum system. The quantum system is described by a wave function rather than a density matrix, for damping and dephasing processes are neglected. Using some assumptions and transformations, we obtain an analytic solution for the wave function. It depends on the pulse-strength parameter and two pulse-shape parameters, as well as the time. Although the wave function has infinitely many components in the continuum limit, taking this limit does not complicate our result. The various features of our result will be shown in later sections, rather than here.

A. *N*-state model

A quantum system having N states is driven by classical oscillating external forces. States 1 and 2 are the discrete states. The continuum is represented by N-2 energy levels with constant spacing $\hbar\Delta$, as shown in Fig. 2. We shall let $N\rightarrow\infty$ at a convenient stage of the calculation, so that the continuum will have no top and no bottom. The continuum will finally be obtained by letting $\Delta\rightarrow 0$.

For this model, the Schrödinger equation contains an $N\times N$ Hamiltonian matrix. This matrix is diagonal in the absence of laser beams, and the energy of each state appears as a diagonal matrix element. The external forces cause oscillating matrix elements to appear off the diagonal. We assume that each laser beam drives only its own transitions, and we use the rotating-wave approximation; this is the explicit form of the assumption about nearly resonant driving forces. In this way, each off-diagonal matrix element of the Hamiltonian becomes zero or a constant multiple of $\exp(\pm i\Omega_L t)$, where Ω_L is one of the laser frequencies. Matrix elements representing the first (second) laser beam appear in the first (second) row and column; see Fig. 2. All other off-diagonal elements of the Hamiltonian matrix are zero.

The laser pulses used for selective excitation are rather long compared to optical periods, and the transformation formulated by Einwohner, Wong, and Garrison [15] is used to remove all optical-frequency terms from the Hamiltonian and wave function. This time-dependent unitary transformation leads to

$$i\frac{d}{dt}\Psi=\mathcal{H}\Psi\ ,$$

where $\hbar=1$, t is the time, and Ψ is a column vector with components $A_1, A_2, \ldots, A_N$. As usual, $|A_j|^2$ is the occupation probability for state j. The Hamiltonian matrix is

$$\mathcal{H}=\begin{bmatrix} -\Delta_1 & 0 & -\frac{1}{2}\Omega_{13} & -\frac{1}{2}\Omega_{14} & \cdots \\ 0 & -\Delta_2 & -\frac{1}{2}\Omega_{23} & -\frac{1}{2}\Omega_{24} & \cdots \\ -\frac{1}{2}\Omega_{13}^* & -\frac{1}{2}\Omega_{23}^* & -\Delta_3 & 0 & \cdots \\ -\frac{1}{2}\Omega_{14}^* & -\frac{1}{2}\Omega_{24}^* & 0 & -\Delta_4 & \cdots \\ \vdots & \vdots & \vdots & \vdots & \end{bmatrix}, \tag{1}$$

where Δ_j is related to the detuning of the two lasers from state j and Ω_{mj} is the Rabi frequency. Ω_{mj} is proportional to the amplitude of the mth optical-frequency field and proportional to the dipole matrix element for the m-j transition. We introduce pulse shapes by allowing Ω_{mj} to depend on t, but it must change slowly compared to optical frequencies. This makes (1) into a time-dependent Hamiltonian matrix. We may choose the phases so that $\Omega_{mj}(t)$ is real. We assume that $\Omega_{mj}(t)$ is independent of j, in order to get a featureless continuum.

Let T be the duration of the two overlapping laser pulses; this means that $\Omega_{mj}(t)=0$ unless $0\le t\le T$. The pulse shape used in our analytic treatment is given by

$$\begin{aligned}\Omega_{1j}(t)&=M\cos\Theta(t)\ ,\\ \Omega_{2j}(t)&=M\sin\Theta(t)\end{aligned} \tag{2}$$

for $j=3,4,\ldots,N$ and $0\le t\le T$. This trigonometric pulse shape is associated with

$$\Delta_1=\Delta_2\ , \tag{3}$$

another simplifying assumption. Assumptions (2) and (3) are suggested by the work of Gottlieb [16] on the three-state model; see also Hioe, Pegg, and Gottlieb [17]. Equation (3) suggests the arrowhead positions in Figs. 1 and 2.

The Schrödinger equation can now be simplified by the

rotation

$$B_1(t)=A_1(t)\cos\Theta(t)+A_2(t)\sin\Theta(t)$$

and

$$B_2(t)=-A_1(t)\sin\Theta(t)+A_2(t)\cos\Theta(t)\ .$$

The new wave function has components $B_1, B_2, A_3, \ldots, A_N$. The new Hamiltonian matrix is

$$H=\begin{bmatrix} -\Delta_1 & id\Theta/dt & -\frac{1}{2}M & -\frac{1}{2}M & \cdots \\ -id\Theta/dt & -\Delta_1 & 0 & 0 & \cdots \\ -\frac{1}{2}M & 0 & -\Delta_3 & 0 & \cdots \\ -\frac{1}{2}M & 0 & 0 & -\Delta_4 & \cdots \\ \vdots & \vdots & \vdots & \vdots & \end{bmatrix} . \quad (4)$$

Here, M is real and the diagonal matrix elements are unchanged by the rotation. We now assume that $d\Theta/dt$ is a constant, so that H is a time-independent matrix. The only difficulty of the computation is putting

$$U(t)=\exp(-iHt) \quad (5)$$

into a convenient form. Any element of this $N\times N$ matrix can be found by the Laplace-transform method of Stey and Gibberd [18]. The limit as $N\to\infty$ is not hard to find if Δ_j has the form suggested by Fig. 2. We may choose $\Delta_3=0$, because one undetermined constant appears in the formulas of Einwohner, Wong, and Garrison [15]. Thus we have

$$\Delta_3=0,\ \Delta_4=\Delta,\ \Delta_5=-\Delta,\ \Delta_6=2\Delta,\ \Delta_7=-2\Delta,\ \cdots,$$

where Δ is the constant spacing shown in Fig. 2. Evaluation of (5) is now only slightly different from the treatment of the first model described by Stey and Gibberd [18]. In the limit as $N\to\infty$, we have

$$U_{11}(t)=\frac{1}{2\pi i}\int_{s_0-i\infty}^{s_0+i\infty}\frac{\exp(st)ds}{s-i\Delta_1+\left[\frac{d\Theta}{dt}\right]^2\Big/(s-i\Delta_1)+\frac{\pi M^2}{4\Delta}\coth\frac{\pi s}{\Delta}}\ , \quad (6)$$

where s_0 is a positive constant, used to keep the path of integration away from the singularities on the imaginary s axis. All other matrix elements of (5) are similarly expressed as inverse Laplace transforms.

Let

$$\Theta(t)=\Theta_0+\beta\left[\frac{2t}{T}-1\right], \quad (7)$$

so that $\Theta(t)$ varies from $\Theta_0-\beta$ to $\Theta_0+\beta$, and $d\Theta/dt=2\beta/T$. The dimensionless pulse-shape parameters are Θ_0 and β, and the dimensionless pulse-strength parameter appears below. The assumption that $\Omega_{mj}(t)\geq 0$ is not necessary, but this natural assumption implies that $M>0$ and that $\Theta(t)$ is an angle in the first quadrant. If so and if $\beta\neq 0$, (2) shows that the Rabi frequencies are increasing and decreasing functions of t; $\beta>0$ gives the intuitive pulse order and $\beta<0$ gives the counterintuitive pulse order. Four cases are shown in Figs. 3 and 4. If $\Theta(t)$ is confined to the first quadrant, then $\Theta_0=\pi/4$ and $\beta=\pm\pi/4$ represent the two extreme cases of intuitive and counterintuitive pairs. In these two extreme cases, one Rabi frequency is zero at the initial time and the other is zero at the final time; see Fig. 3(a). These extreme cases were treated in our recent paper [19]. Here, we give the result for the more general case. Some examples of the two Rabi frequencies are shown in Figs. 3 and 4. For the case of $\beta=0$, we have two rectangular pulses that start and end simultaneously; this special case is examined in Sec. VI.

The initial time is $t=0$, and we assume that the quantum system is initially in state 1. The initial conditions we use are $A_1(0)=1$ and $A_j(0)=0$ for $j\geq 2$. Since T is the duration of the two overlapping laser pulses, we evaluate (5) only for $t\leq T$. Evaluation of (6) and similar integrals is relatively simple if we assume $T<2\pi/\Delta$. Since we are interested in the limit as $\Delta\to 0$, this assumption is hardly a restriction. The hyperbolic cotangent appearing in (6) can now be replaced by unity. This is shown by variation of s_0; see Stey and Gibberd [18]. Hence,

$$U_{11}(t)=\left[\cosh(Rt)-\frac{\pi M^2}{8\Delta R}\sinh(Rt)\right]\times\exp\left[i\Delta_1 t-\frac{\pi M^2}{8\Delta}t\right],$$

$$U_{12}(t)=\frac{2\beta}{RT}\sinh(Rt)\exp\left[i\Delta_1 t-\frac{\pi M^2}{8\Delta}t\right],$$

and so forth. Here,

$$R=\left[\left[\frac{\pi M^2}{8\Delta}\right]^2-\left[\frac{d\Theta}{dt}\right]^2\right]^{1/2}$$

is a frequency that can be positive, zero, or imaginary. The initial conditions are such that we need $U_{jk}(t)$ only for $k=1$ and 2.

The solution of (1) is now given by

$$A_1(t)=\left[\cosh(Rt)\cos[\Theta(t)-\Theta_0+\beta]-\frac{\pi M^2}{8\Delta R}\sinh(Rt)\cos[\Theta(t)+\Theta_0-\beta]+\frac{2\beta}{RT}\sinh(Rt)\sin[\Theta(t)-\Theta_0+\beta]\right]\times\exp\left[i\Delta_1 t-\frac{\pi M^2}{8\Delta}t\right],$$

and so forth. These time-dependent probability amplitudes should be expressed in terms of dimensionless quantities, such as t/T. The dimensionless pulse-strength parameter used here is

$$x=\frac{\pi M^2 T}{8\Delta} . \tag{8}$$

We find

$$A_1(t)=\left[\cosh(Rt)\cos(2\beta t/T) -x\frac{\sinh(Rt)}{RT}\cos[2\Theta_0+2\beta(t/T-1)] +2\beta\frac{\sinh(Rt)}{RT}\sin(2\beta t/T)\right]\exp\left[i\Delta_1 t-\frac{xt}{T}\right] \tag{9}$$

and

$$A_2(t)=\left[\cosh(Rt)\sin(2\beta t/T) -x\frac{\sinh(Rt)}{RT}\sin[2\Theta_0+2\beta(t/T-1)] -2\beta\frac{\sinh(Rt)}{RT}\cos(2\beta t/T)\right]\exp\left[i\Delta_1 t-\frac{xt}{T}\right] , \tag{10}$$

where $RT=(x^2-4\beta^2)^{1/2}$ appears as an auxiliary dimensionless parameter. For $j\geq 3$, we find

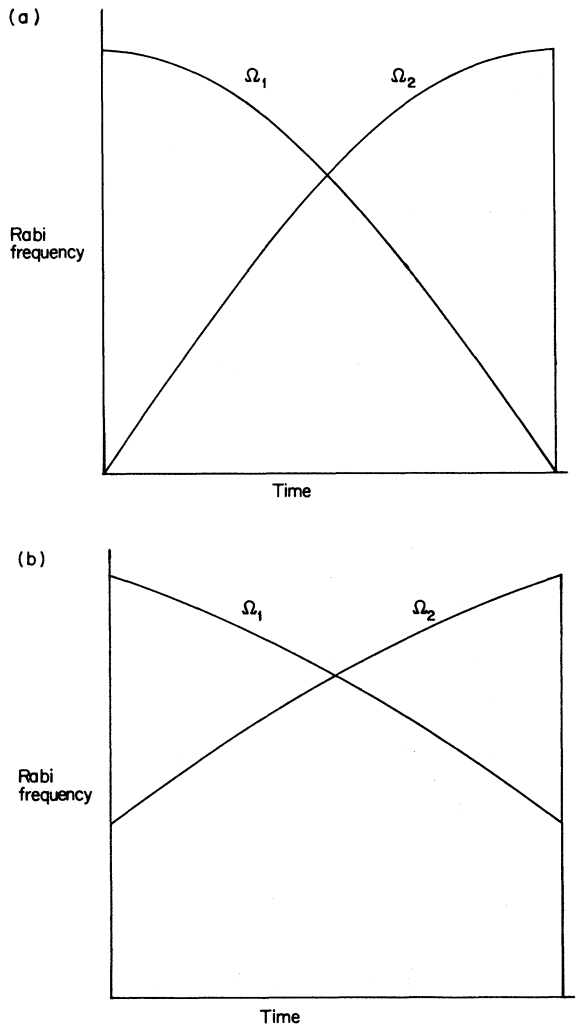

FIG. 3. Examples of Rabi frequencies given by Eqs. (2) and (7) for $\Theta_0=\pi/4$, and (a) $\beta=\pi/4$, (b) $\beta=\pi/8$. The labels 1 and 2 for the two pulses are interchanged when β changes its sign from positive to negative. The pairs of Rabi frequencies have equal maximum and minimum values.

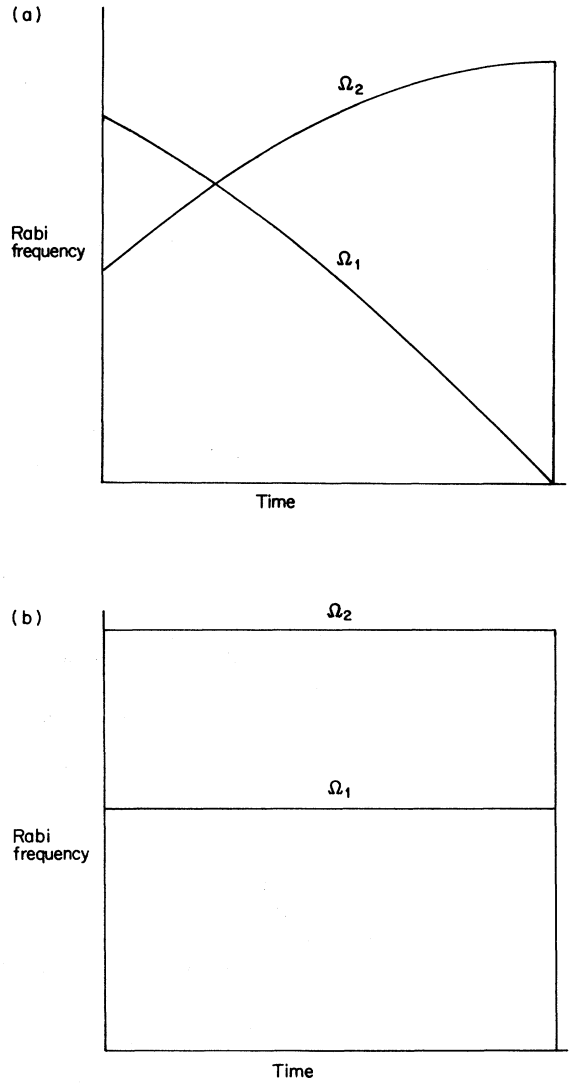

FIG. 4. Examples of Rabi frequencies given by Eqs. (2) and (7) for $\Theta_0=\pi/3$, and (a) $\beta=\pi/6$ and (b) $\beta=0$. The pairs of Rabi frequencies have different maximum and minimum values.

$$A_j(t)=\frac{(\frac{1}{2}MT)[\delta\cos(\Theta_0-\beta)+2i\beta\sin(\Theta_0-\beta)]}{\delta^2-4\beta^2-2ix\delta}\exp(i\Delta_j t)$$
$$+\frac{(\frac{1}{2}MT)\left[-\delta\cosh(Rt)+(x\delta-4i\beta^2)\frac{\sinh(Rt)}{RT}\right]\cos(\Theta_0-\beta)}{\delta^2-4\beta^2-2ix\delta}\exp\left[i\Delta_1 t-\frac{xt}{T}\right]$$
$$+\frac{(\frac{1}{2}MT)(-2i\beta)\left[\cosh(Rt)+(x+i\delta)\frac{\sinh(Rt)}{RT}\right]\sin(\Theta_0-\beta)}{\delta^2-4\beta^2-2ix\delta}\exp\left[i\Delta_1 t-\frac{xt}{T}\right], \tag{11}$$

where

$$\delta=T(\Delta_j-\Delta_1) \tag{12}$$

is the dimensionless detuning parameter used to label places in the continuum.

B. Continuum limit

We can now complete this calculation by taking the continuum limit. The results will be written in terms of t/T, Θ_0, β, x, and δ, dimensionless parameters that are meaningful in the continuum limit; the last four of them are defined by (7), (8), and (12). We let $\Delta\to 0$, but this is only part of this limiting process. If a large box is used to discuss the continuum [20], each continuum wave function approaches zero as the size of the box increases. Hence, the transition dipole matrix elements and the Rabi frequencies also approach zero. This means that M and (11) both vanish in the limit; the occupation probability of any one continuum state is zero. Further consideration of continuum wave functions shows that (8) approaches a nonzero limit as the size of the box increases. If we neglect changes in M^2/Δ and (8) as the size of the box increases, then (9) and (10) contain nothing that depends on the size of the box. The remaining calculation is only the treatment of the continuum states. We find the density of occupation probability in the continuum before calculating the total occupation probability of the continuum. The probability density for energies in the continuum is $|A_j(t)|^2/\Delta$, but we use (12), rather than energy or j, to label places in the continuum. The probability density for this dimensionless detuning is

$$P_\delta(t)=|A_j(t)|^2/\Delta T, \tag{13}$$

and $\int P_\delta(t)d\delta$ is the occupation probability for a part of the continuum at time t. The explicit formula is

$$P_\delta(t)=\frac{2x}{\pi|\delta^2-4\beta^2-2ix\delta|^2}\left|[\delta\cos(\Theta_0-\beta)+2i\beta\sin(\Theta_0-\beta)]\left[\exp\frac{i\delta t}{T}-\cosh(Rt)\exp\left[-\frac{xt}{T}\right]\right]\right.$$
$$\left.+[(x\delta-4i\beta^2)\cos(\Theta_0-\beta)-2i\beta(x+i\delta)\sin(\Theta_0-\beta)]\frac{\sinh(Rt)}{RT}\exp\left[-\frac{xt}{T}\right]\right|^2, \tag{14}$$

where j does not appear. We can now verify that

$$|A_1(t)|^2+|A_2(t)|^2+\int_{-\infty}^{\infty}P_\delta(t)d\delta=1. \tag{15}$$

This lengthy calculation is simplified by use of the residue calculus. It shows that the occupation probabilities always sum to unity.

We notice a peculiar feature of the present continuum limit. The quantities (9), (10), and (13) are constant as Δ and M approach zero, provided that small changes in M^2/Δ are neglected and $\Delta T<2\pi$; this last inequality was used to simplify the evaluation of (5). The replacement of j by δ and the change from (11) to (14) can be regarded as changes of notation, rather than a limiting process.

Finally, the calculated occupation probabilities for state 1, state 2, and the continuum are $|A_1(t)|^2$, $|A_2(t)|^2$, and $1-|A_1(t)|^2-|A_2(t)|^2$. These three probabilities are easily obtained from (9) and (10). They are entirely independent of (3), the detuning of the two laser beams; this confirms that our model has a featureless continuum. These occupation probabilities are discussed in the following two sections. The density of occupation probability in the continuum is given by (14), and is discussed in Sec. V.

III. TIME-DEPENDENT OCCUPATION PROBABILITIES

The transition rate given by our calculation should be compared with the golden rule of time-dependent perturbation theory [20], and we find agreement at times near the start of the two overlapping laser pulses. The maximum occupation probability for the continuum is also considered in this section, for it involves time-dependent probabilities.

State 1 is initially occupied with unit probability. The initial decay of this occupation probability is described by

$$|A_1(t)|^2=1-4x(t/T)\cos^2(\Theta_0-\beta)+\cdots, \tag{16}$$

where the square and higher powers of t/T are not shown. The initial decay rate of this quantity is given

correctly by the golden rule of time-dependent perturbation theory [20], which is applied as follows. In (1), the matrix element for the transition from state 1 to the continuum is $-\frac{1}{2}M\cos(\Theta_0-\beta)$. Also, the density of continuum states is $1/\Delta$, and $\hbar=1$. Hence, the initial decay rate of (16) should be

$$2\pi|-\tfrac{1}{2}M\cos(\Theta_0-\beta)|^2\frac{1}{\Delta}=\frac{4x}{T}\cos^2(\Theta_0-\beta)\ ,$$

where x is defined by (8). This simple calculation agrees with (16), and it explains the meaning of (8). This connection with perturbation theory could be used to connect our calculation with detailed information on the transition matrix elements for a specific molecule or atom.

The time-dependent occupation probability of the continuum is of interest here, because spontaneous emission is likely to limit the application of selective excitation via the continuum. This occupation probability is $1-|A_1(t)|^2-|A_2(t)|^2$, and the Appendix shows that it is an increasing function of t. Hence, it is maximum at $t=T$. We have reason to look at $1-|A_1(T)|^2-|A_2(T)|^2$, and this occupation probability can be small. It is considered in the following section.

IV. FINAL OCCUPATION PROBABILITIES

The two overlapping laser pulses end at $t=T$, and the occupation probabilities at this final time are examined in this section. We give particular attention to the final occupation probability for state 2, because this is an obvious test of selectivity of the excitation process.

The final occupation probabilities for states 1 and 2 are easily obtained from (9) and (10):

$$|A_1(T)|^2=[\cos(2\beta)C(x,\beta)-x\cos(2\Theta_0)S(x,\beta)+2\beta\sin(2\beta)S(x,\beta)]^2$$

and

$$|A_2(T)|^2=[\sin(2\beta)C(x,\beta)-x\sin(2\Theta_0)S(x,\beta)-2\beta\cos(2\beta)S(x,\beta)]^2\ . \tag{17}$$

Here, $C(x,\beta)=\cosh(RT)\exp(-x)$ and $S(x,\beta)=[\sinh(RT)/RT]\exp(-x)$ are positive quantities even when $RT=(x^2-4\beta^2)^{1/2}$ is imaginary. We recall that β and Θ_0 are pulse-shape parameters; see Fig. 3 and 4.

Since our main purpose is study of coherent transfer to state 2, we now maximize (17). In the first place, (17) has a simple and explicit dependence on Θ_0, and its maximum must be at $\sin(2\Theta_0)=\pm1$. The sign is not easily determined, but changing the signs of both Θ_0 and β does not change the value of (17); it changes only an unimportant sign in (1). Hence, we emphasize the case of $\sin(2\Theta_0)=1$ and

$$\Theta_0=\pi/4\ . \tag{18}$$

If the condition $\Omega_{mj}(t)\geq0$ is imposed, we derive (18) from a different argument. The condition (18) implies that the values of the two Rabi frequencies are interchanged if we replace t by $T-t$; see Fig. 3.

The final occupation probability of state 2 is plotted in Fig. 5. The maximum of $|A_2(T)|^2$ is always found at $\Theta_0=\pi/4$ and at a negative value of β; if $x\geq2.1$, it is found at $\beta<-\pi/6$. Although a much wider variety of pulse shapes should be studied, this calculation suggests that the counterintuitive pulse order is always better for the transfer of occupation probability to state 2. Furthermore, the final occupation probability of state 2 can be insensitive to small changes in β or Θ_0; see Fig. 5. Small changes in x will be considered shortly.

The special intuitive and counterintuitive cases of $\Theta_0=\pi/4$ and $\beta=\pm\pi/4$ were mentioned below (7); they are the extreme cases if $\Omega_{mj}(t)\geq0$ is required. Since $C(x,\beta)$ and $S(x,\beta)$ are even functions of β, the two final occupation probabilities for these two extreme cases are

$$|A_1(T)|^2=[\tfrac{1}{2}\pi S(x,\pi/4)]^2$$

and

$$|A_2(T)|^2=[C(x,\pi/4)\mp xS(x,\pi/4)]^2\ ,$$

respectively. These three functions of x are plotted in Fig. 6, which shows a dramatic difference between intuitive and counterintuitive pulse orders. When x is large, these two pulse orders give

$$|A_2(T)|^2=\frac{\pi^4}{2^8x^4}-\frac{\pi^6}{2^{10}x^5}+\cdots$$

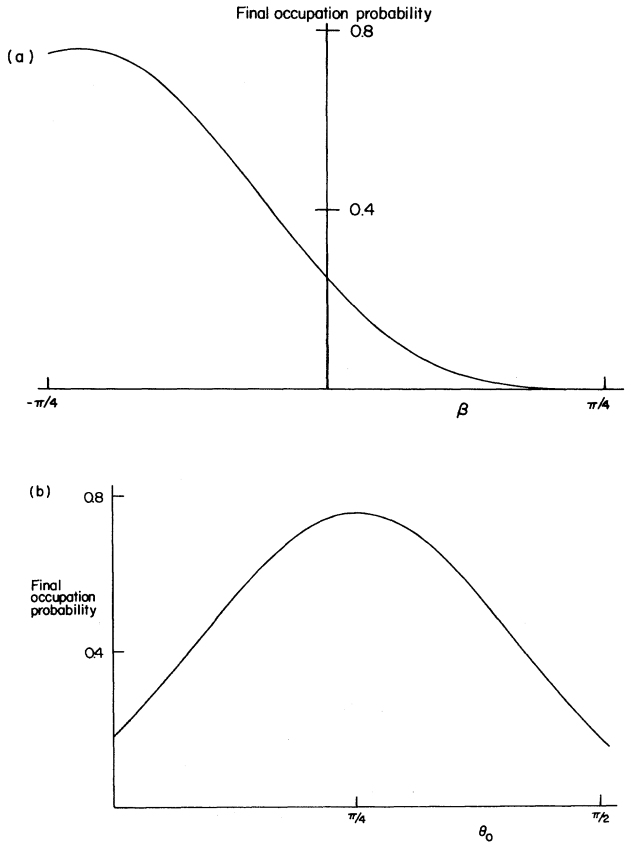

FIG. 5. Final occupation probability of state 2 (a) for $x=8$ and $\Theta_0=\pi/4$ and (b) for $x=8$ and $\beta=-0.6977$.

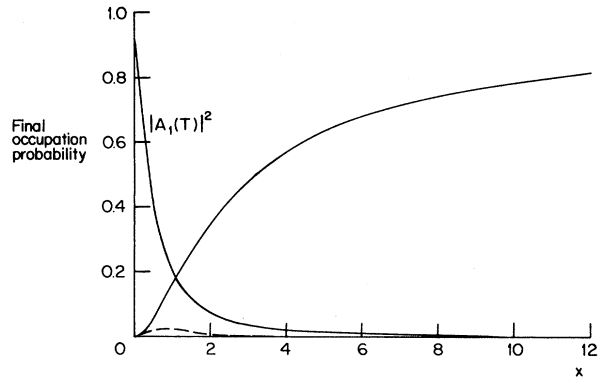

FIG. 6. Final occupation probability $|A_1(T)|^2$ of state 1, for both extreme intuitive and counterintuitive orders, and final occupation probabilities of state 2, for the extreme intuitive order (dashed curve), and for the extreme counterintuitive order (unlabeled solid curve).

and

$$|A_2(T)|^2=1-\frac{\pi^2}{4x}+\frac{\pi^2(\pi^2+4)}{32x^2}+\cdots, \tag{19}$$

respectively. Since the slope of this last function decreases as x increases, the counterintuitive order can be used to make $|A_2(T)|^2$ insensitive to small changes in x. The series (19) and the rising curve in Fig. 6 are valid only for $\beta=-\pi/4$, and a different value of β would give a larger final occupation probability for state 2. However, the difference is quite small if x is greater than a few units.

The final occupation probability for state 2 approaches unity as the pulse-strength parameter increases, according to (19). We expect this limit to be unity in calculations for any simple pulse shape and any detuning, if one uses the counterintuitive pulse order and neglects relaxation effects. We can cite calculations for no other continuum model, but some calculations for three-state models should be mentioned. Suppose that $N=3$, so that (1) and (4) are 3×3 matrices. If $\Theta_0=\pi/4$ and $\beta=-\pi/4$, computation of $|A_2(T)|^2$ is straightforward, regardless of whether (3) vanishes. Furthermore, we use the results for a three-state model [8] having pulse shapes greatly different from those in this paper. Both sets of results support the claim that the counterintuitive pulse order gives $|A_2(T)|^2\rightarrow1$ as the pulse strength is increased.

The great advantage of the counterintuitive pulse order for transfer to the desired final state has been shown in this section; see figs. 5(a) and 6. Furthermore, the maximum occupation probability of the continuum, which is treated in Sec. III and the Appendix, can be kept small by use of the counterintuitive pulse order. This tends to justify our neglect of spontaneous emission, dephasing of continuum states, and stimulated continuum-continuum transitions. Finally, Figs. 5 and 6 show that the final occupation probability for state 2 can be insensitive to small changes in the dimensionless parameters of the pulse pair.

V. DISTRIBUTION OF OCCUPATION PROBABILITY IN THE CONTINUUM

This distribution has a width that we notice in this section, and it can show many bumps or maxima. Although the probability density for this distribution is given explicitly by (14), some features of this formula should be brought out.

For large detunings, the probability density falls off, following ultimately an inverse-square law. This is seen by making $\delta\rightarrow\pm\infty$ in (14). The width of the energy distribution is ordinarily roughly the same as the transition

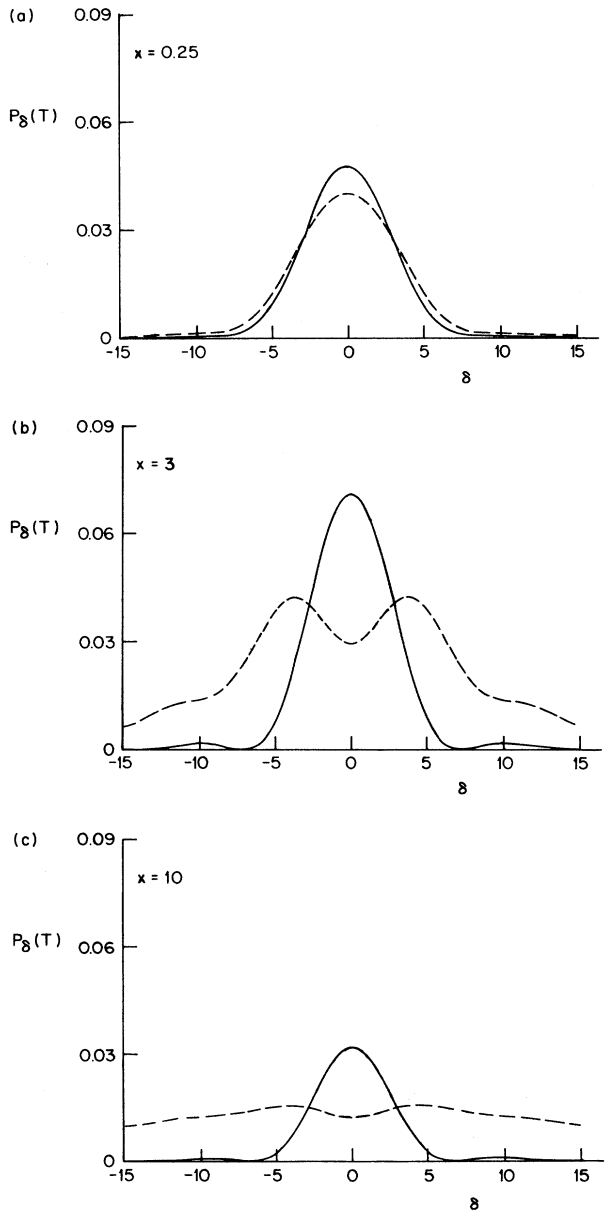

FIG. 7. Density of occupation probability in the continuum at end of overlapping laser pulses for three different values of x, the dimensionless pulse strength. The solid curve is for the extreme counterintuitive order and the dashed curve is for the extreme intuitive order.

rate given by the golden rule, which is of the order of M^2/Δ. When the dimensionless variables (8) and (12) are used, the probability density has a value roughly similar to the peak value until $|\delta| \gg x$, if x is large. Although our continuum model is topless and bottomless, the populated continuum states are found only at detunings that are small compared to optical frequencies. Furthermore, the counterintuitive pulse order can be used to make the wings of this distribution much weaker. This difference is shown in Fig. 7, and it can be derived from (14). In the extreme counterintuitive case of $\Theta_0=\pi/4$ and $\beta=-\pi/4$, $\cos(\Theta_0-\beta)=0$ and (14) gives

$$P_\delta(T)=\frac{\pi x}{2\delta^2}[S(x,\pi/4)]^2+O\left[\frac{1}{\delta^3}\right]+\cdots . \tag{20}$$

Then, $x \gg 1$ gives $S(x,\pi/4)\approx 1/2x$, so that the probability density in the wings is (constant)$/x\delta^2$. However, if $\cos(\Theta_0-\beta)$ is much different from zero, then the population transfer out of the initial state starts suddenly. If so, the $[S(x,\pi/4)]^2$ appearing in (20) is replaced by a number of order unity, and $P_\delta(T)$ is not so small in the wings. This is shown in Fig. 7 for the extreme intuitive case for which $\Theta_0=\pi/4$, $\beta=\pi/4$, and $\cos(\Theta_0-\beta)=1$. If $x<1$, this contrast is not found; small values of x kill the great difference between intuitive and counterintuitive pulse orders.

The distribution of occupation probability in the continuum shows many maxima in some cases. These maxima occur at energies separated approximately by multiples of $2\pi/T$. When the dimensionless variable (12) is used as the abscissa, the maxima are separated approximately by multiples of 2π; see Fig. 7. Large-scale plots of this distribution can be used to distinguish maxima from other bumps.

This brief discussion of (14) has shown another difference between intuitive and counterintuitive pulse orders. If the pulse strength is moderately large, the intuitive pulse order can be used to transfer most of the occupation probability from state 1 to the continuum, and to spread it out over a relatively wide band of continuum energies; see Figs. 6 and 7. On the other hand, if the counterintuitive pulse order is used, the maximum occupation probability of the continuum is 0.6311, which occurs at $x=1.0992$, and the population in the continuum is spread over only a narrow band of continuum energies when x is large. Furthermore, the population in the continuum decreases to zero as x increases.

VI. RECTANGULAR PULSE SHAPE

We have used laser pulse shapes given by (2), where $\Theta(t)$ is an increasing or decreasing function of t. In this section, we make $\Theta(t)$ constant, in order to connect our calculation with simple models of coherent population trapping and ionization suppression, two phenomena which may be closely related [13].

The two laser pulses begin at $t=0$ and end at $t=T$. Let $d\Theta/dt=0$ or $\beta=0$, so that the pulse shapes given by (2) are rectangular. The Rabi frequencies during this time interval are constants equal to $M\cos\Theta_0$ and $M\sin\Theta_0$. Two such Rabi frequencies could arise from a single rectangular pulse driving both of the discrete-continuum transitions, if states 1 and 2 have nearly the same energy; in fact, they must have precisely the same energy, because (3) is assumed. Since $\beta=0$ implies $RT=x$, (9) and (10) give

$$|A_1(t)|^2=[(\sin\Theta_0)^2+(\cos\Theta_0)^2\exp(-2xt/T)]^2 \tag{21a}$$

and

$$|A_2(t)|^2=(\sin\Theta_0\cos\Theta_0)^2[1-\exp(-2xt/T)]^2 . \tag{21b}$$

Using (15), we find that the occupation probability of the continuum is

$$\int_{-\infty}^{\infty} P_\delta(t)d\delta=(\cos\Theta_0)^2[1-\exp(-4xt/T)] . \tag{21c}$$

These occupations probabilities agree with those found by Parker and Stroud [13] in one of their calculations. In order to make connection with their notation, we notice that the golden rule gives $2\Gamma_1=(4x/T)\cos^2\Theta_0$ or $2\Gamma_2=(4x/T)\sin^2\Theta_0$ as the transition rate for a quantum system that is known to be in state 1 or state 2, respectively. Using these values of Γ_1 and Γ_2, and the rectangular pulse shape, we find that (21a) and (21b) agree with Eqs. (10) and (9) of Ref. [13].

Each of the occupation probabilities (21) shows a physical effect of the rectangular pulse shape. From (21a), $|A_1(T)|^2$ is never less than $\sin^4\Theta_0$; we may say that population trapping occurs unless $\sin\Theta_0=0$. If $\sin\Theta_0=0$, state 2 is completely decoupled from other states, we have purely exponential decay of $|A_1(t)|^2$, and the time constant agrees with that obtained from the golden rule.

From (21b), $|A_2(t)|^2$ is never greater than $(\frac{1}{4})\sin^2(2\Theta_0)$, and this value is reached only for strong laser pulses. The greatest transfer to state 2 is obtained at $\Theta_0=\pi/4$, where the couplings of states 1 and 2 to the continuum are equally strong.

From (21c), the occupation probability of the continuum is never greater than $\cos^2\Theta_0$, and this value is reached only for strong laser pulses. This maximum value is less than unity, except when $\sin\Theta_0=0$ and state 2 is decoupled from other states. Either this maximum occupation probability for the continuum or $|A_1(T)|^2 \geq \sin^4\Theta_0$ can be regarded as evidence of ionization suppression, but see other explanations [14].

The occupation probabilities given by (21) should be compared with those found for the three-state model used by Gray, Whitley, and Stroud [11] to explain their population-trapping experiment. If we make (1) into a 3×3 matrix and set all detunings equal to zero, the time-dependent occupation probabilities become

$$|A_1(t)|^2=[(\sin\Theta_0)^2+(\cos\Theta_0)^2\cos(\tfrac{1}{2}Mt)]^2 ,$$

$$|A_2(t)|^2=(\sin\Theta_0\cos\Theta_0)^2(1-\cos\tfrac{1}{2}Mt)^2 ,$$

and

$$|A_3(t)|^2=[\cos\Theta_0\sin(\tfrac{1}{2}Mt)]^2 , \tag{22}$$

where state 3 has replaced the continuum and $\cos\frac{1}{2}Mt$ has replaced $\exp(-2xt/T)$. The occupation probability of state 3 is never greater than $\cos^2\Theta_0$, and this agrees

with the corresponding result for the continuum model. However, the maximum value of (22) is attained whenever $\cos(\frac{1}{2}Mt)=0$, and (22) oscillates as M increases, rather than approaching a limit as the laser pulse becomes stronger.

The final occupation probability of state 1 can be zero even if $\sin\Theta_0\neq 0$. The minimum occupation probability of state 1 is $[\min(0, \cos 2\Theta_0)]^2$. The occupation probability of state 2 is never greater than $\sin^2(2\Theta_0)$, which can be unity. Complete transfer to state 2 is obtained if $\Theta_0=\pi/4$ and $\cos(\frac{1}{2}MT)=-1$. These results are quite different from those for the continuum model.

VII. CONCLUSION

We have treated a model for laser-driven coherent transfer from state 1 to the continuum to state 2. We have shown that a significant amount of population can be transferred from state 1 to state 2 if two overlapping laser pulses arranged in the counterintuitive order are used. We have also shown the great differences between the results for the intuitive and counterintuitive pulse orders. The special case in which the two transitions to the continuum are driven by one rectangular laser pulse has been used to connect this calculation with ionization suppression.

APPENDIX

In our model, the occupation probability for the continuum increases with time, until the end of the overlapping laser pulses. This is shown by the following calculation. Since (15) holds, we have to show that

$$|A_1(t)|^2+|A_2(t)|^2 = \left[\frac{x^2+2\beta x\sin(2\Theta_0-2\beta)}{x^2-4\beta^2}\cosh(2Rt) - \frac{x}{RT}\cos(2\Theta_0-2\beta)\sinh(2Rt) - \frac{4\beta^2+2\beta x\sin(2\Theta_0-2\beta)}{x^2-4\beta^2}\right]\exp\left[-\frac{2xt}{T}\right] \quad \text{(A1)}$$

is a decreasing function of t. The time derivative of this expression is easily computed, and the related dimensionless quantity is

$$T\frac{d}{dt}[|A_1(t)|^2+|A_2(t)|^2] = -2x\left\{\frac{x^2\cosh(2Rt)-4\beta^2}{x^2-4\beta^2}-\frac{x}{RT}\sinh(2Rt) + \frac{2\beta}{RT}\left[\frac{x}{RT}\cosh(2Rt)-\frac{x}{RT}-\sinh(2Rt)\right]\sin(2\Theta_0-2\beta) + \left[\cosh(2Rt)-\frac{x}{RT}\sinh(2Rt)\right]\cos(2\Theta_0-2\beta)\right\}\exp-\frac{2xt}{T}\,.$$

The quantity in braces is positive at all times, with possible one exception. This holds because

$$\frac{x^2\cosh(2Rt)-4\beta^2}{x^2-4\beta^2}-\frac{x}{RT}\sinh(2Rt) \quad \text{(A2)}$$

is a positive quantity, and the other terms can easily be bounded. The sum of the squares of the coefficients of $\sin(2\Theta_0-2\beta)$ and $\cos(2\Theta_0-2\beta)$ is equal to the square of (A2). Hence, the quantity in braces is positive, except that it can be zero when the coefficients of $\sin(2\Theta_0-2\beta)$ and $\cos(2\Theta_0-2\beta)$ have a ratio of $\tan(2\Theta_0-2\beta)$. However, this ratio of the coefficients is certainly time dependent. Even if the derivative vanishes at one time, (A1) is a decreasing function of the time. This argument needs only a slight modification if RT is imaginary. The special case of $RT=0$ need not be treated explicitly in this Appendix nor elsewhere in the paper.

[1] C. Liedenbaum, S. Stolte, and J. Reuss, Phys. Rep. **178**, 1 (1989).

[2] Special Issue on Stimulated-Emission Pumping, edited by Hai-Lung Dai, J. Opt. Soc. Am. B **7**, 1801 (1990).

[3] U. Gaubatz, P. Rudecki, S. Schiemann, and K. Bergmann, J. Chem. Phys. **92**, 5363 (1990).

[4] H. -G. Rubahn, E. Konz, S. Schiemann, and K. Bergmann, Z. Phys. D **22**, 401 (1991).

[5] P. Marte, P. Zoller, and J. L. Hall, Phys. Rev. A **44**, 4118 (1991).

[6] U. Gaubatz, P. Rudecki, M. Becker, S. Schiemann, M. Külz, and K. Bergmann, Chem. Phys. Lett. **149**, 463 (1988); C. Liedenbaum, S. Stolte, and J. Reuss, Infrared Phys. **29**, 397 (1989).

[7] J. R. Kuklinski, U. Gaubatz, F. T. Hioe, and K. Bergmann, Phys. Rev. A **40**, 6741 (1989); C. E. Carroll and F. T. Hioe, *ibid.* **42**, 1522 (1990); G. Z. He, A. Kuhn, S. Schiemann, and K. Bergmann, J. Opt. Soc. Am. B **7**, 1960 (1990); G. W. Coulston and K. Bergmann, J. Chem. Phys. **96**, 3467 (1992); A. Kuhn, G. W. Coulston, G. Z. He, S. Schiemann, and K. Bergmann, *ibid.* **96**, 4215 (1992).

[8] C. E. Carroll and F. T. Hioe, J. Phys. B **22**, 2633 (1989).

[9] J. Oreg, F. T. Hioe, and J. H. Eberly, Phys. Rev. A **29**, 690 (1984); F. T. Hioe, Phys. Lett. A **99**, 150 (1983); C. E. Car-

roll and F. T. Hioe, J. Opt. Soc. Am. B **5**, 1335 (1988).
[10] E. Arimondo and G. Orriols, Lett. Nuovo Cimento **17**, 333 (1976); P. M. Radmore and P. L. Knight, J. Phys. B **15**, 561 (1982).
[11] H. R. Gray, R. M. Whitley, and C. R. Stroud, Jr., Opt. Lett. **3**, 218 (1978).
[12] R. R. Jones and P. H. Bucksbaum, Phys. Rev. Lett. **67**, 3215 (1991); L. D. Noordam, H. Stapelfeldt, D. I. Duncan, and T. F. Gallagher, Phys. Rev. Lett. **68**, 1496 (1992).
[13] J. Parker and C. R. Stroud, Jr., Phys. Rev. A **41**, 1602 (1990).
[14] E. Kyrölä and J. H. Eberly, J. Chem. Phys. **82**, 1841 (1985); M. V. Fedorov and A. M. Movsesian, J. Opt. Soc. Am. B **6**, 928 (1989); Q. Su, J. H. Eberly, and J. Javanainen, Phys. Rev. Lett. **64**, 862 (1990); R. Grobe and C. K. Law, Phys. Rev. A **44**, 4114 (1991); S. Geltman, *ibid.* **45**, 5293 (1992).
[15] T. H. Einwohner, J. Wong, and J. C. Garrison, Phys. Rev. A **14**, 1452 (1976).
[16] H. P. W. Gottlieb, Phys. Rev. A **26**, 3713 (1982).
[17] F. T. Hioe, Phys. Rev. A **29**, 3434 (1984); D. T. Pegg, J. Phys. B **18**, 415 (1985); H. P. W. Gottlieb, Phys. Rev. A **32**, 653 (1985).
[18] G. C. Stey and R. W. Gibberd, Physica **60**, 1 (1972).
[19] C. E. Carroll and F. T. Hioe, Phys. Rev. Lett. **68**, 3523 (1992).
[20] D. Bohm, *Quantum Theory* (Prentice-Hall, New York, 1951); L. I. Schiff, *Quantum Mechanics* (McGraw-Hill, New York, 1949).